A R C H I V E S O F M E T A L L U R G Y A N D M A T E R I A L S
Volume 53 2008 Issue 1

P. PANEK*, K. DRABCZYK*, H. CZTERNASTEK **, E. KUSIOR**, P. ZIĘBA*, E. BEŁTOWSKA-LEHMAN*

THE INFLUENCE OF SURFACE TEXTURE AND TEMPARATURE DEPOSITION OF TiO_2 LAYER ON CRYSTALLINE SILICON SOLAR CELLS PARAMETERS

WPŁYW TEKSTURY POWIERZCHNIOWEJ I TEMPERATURY OSADZANIA WARSTWY TiO_2 NA PARAMETRY KRZEMOWYCH KRYSTALICZNYCH OGNIW SŁONECZNYCH

In the present work, the investigation of the titanium dioxide (TiO_2) thin layer as an antireflection coating for silicon solar cells are presented. The TiO_2 layers were obtained by the chemical vapour deposition method using tetraethylorthotitanat $(C_2H_5O)Ti$ at temperatures of the silicon wafers in the range from 150°C to 400°C. It has been established that all of the obtained TiO_2 layers contain anatase phase embedded in the amorphous background. A progress of the crystallization process with the increasing temperature of the substrate during the deposition has been observed. The change in opto-electronic parameters of silicon solar cells as a function of the deposition temperature of the antireflection coating has been discussed, taking into account the evolution of the crystallographic structure.

Keywords: titanium dioxide, antireflection coating, crystalline silicon solar cell

Praca przedstawia wyniki badań poświęconych zastosowaniu cienkich warstw TiO_2 jako powłok antyrefleksyjnych dla krzemowych ogniw słonecznych. Warstwy TiO_2 wytwarzano metodą chemicznego osadzania z fazy gazowej (CVD) ze źródła ortotytanianutetraetylu $(C_2H_5O)Ti$ w zakresie temperatur płytek krzemowych od 150°C do 400°C. Stwierdzono, że wszystkie otrzymane warstwy TiO_2 charakteryzowały się amorficzną strukturą z wbudowaną fazą anatazu. Zaobserwowano zwiększenie udziału fazy krystalicznej ze wzrostem temperatury krzemowego podłoża. Określono i przedyskutowano zmiany wartości parametrów opto-elektronicznych krzemowych ogniw słonecznych w funkcji temperatury osadzania warstw antyrefleksyjnych TiO_2.

1. Introduction

Global production of solar cells continued its phenomenal growth, reached 2.520 GWp in 2006 year. The mono (Cz-Si) – and multicrystalline (mc-Si) silicon as a basis material continues to dominate the photovoltaic sector taking share 38% and 47%, respectively [1]. Advanced technology of the silicon solar cells requires surface structures enabling reduction of effective front reflection from 34.8%, for planar as-cut Si wafer below 10% in the range of 400–1100 nm electromagnetic radiation. On the other hand, the industrial application needs first of all high output with a low cost which eliminates many techniques and materials.

There are two main methods used in solar cells field and photovoltaic industry for the Si surface reflectance reduction – surface texturization (see Fig. 2) and antireflection coating deposition (ARC). The ARC plays a very important role in silicon solar cell production because of two main reasons: reduction of reflectivity and possibility to obtain good ohmic contact for front electrode simultaneously prevention of Si surface from contamination during co-firing process of front and back contacts. The widely applied in the industry are silicon nitride and titanium dioxide, this last one in low cost silicon solar cells, because the technology of deposition is very simple and easily, can be transferred to a production line without incurring high cost.

2. Experimental procedure

The silicon wafers were (100) Cz-Si, boron doped, p-type, 1 Ω·cm resistivity, 300 μm thick wafers denoted as samples Nos. 1 to 6 and mc-Si, boron doped, p-type,

* INSTITUTE OF METALLURGY AND MATERIALS SCIENCE, POLISH ACADEMY OF SCIENCES, 30-059 KRAKÓW, 25 REYMONTA STR., POLAND
** FACULTY OF ELECTRIC ENGINEERING, AUTOMATICS, COMPUTER SCIENCE AND ELECTRONICS, AGH – UNIVERSITY OF SCIENCE AND TECHNOLOGY, 30-059 KRAKÓW, 30 MICKIEWICZA AV., POLAND

1 Ω·cm resistivity, 300 μm thick as samples Nos. 7 to 12. This kind of Si wafers is used in mass scale industrial manufacturing of the silicon solar cells [2]. All samples were first etched in KOH(30%) to remove the saw damage of the material (10 μm thick from each side of wafers) and texturized in IPA:KOH(40%):DIH$_2$O in volume ratio 3:1:46 solution at 80°C for 15 min. and after that rinsed in HCl(2%) and HF(10%). All chemical processes were completed by rinsing in deionized water and drying in N_2. The emitter with the sheet resistance 40 Ω/□ was generated in an open quartz tube using liquid $POCl_3$ as the doping source, at temperature 840°C for 30 min. After diffusion the parasitic junction was removed by means a special Teflon clamp in which the wafers were immersed in HNO_3(65%):HF(40%):CH_3COOH(80%) solution in the volume ratio 5:3:3 for 1 min. Then phosphorus silicate glass was removed by immersion in a bath of HF(10%) for 2 min. The surface passivation was achieved by the growth of ~10 nm thick SiO_2 layer at the temperature of 800°C for 15 min in a controled O_2 and N_2 atmosphere.

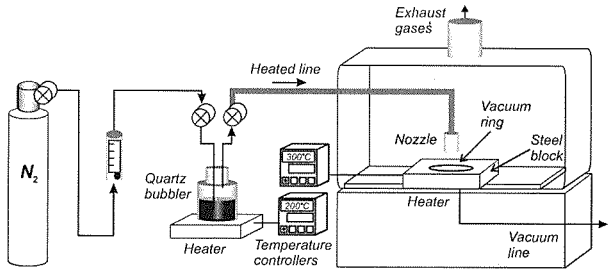

Fig. 1. Scheme of the TiO_2 antireflection layer deposition system by CVD method

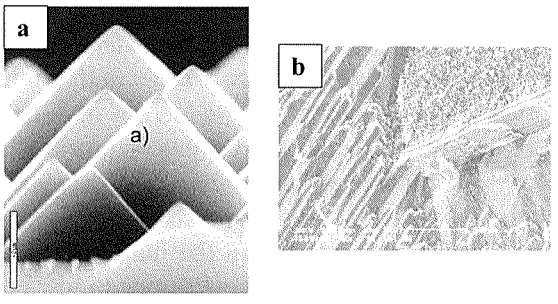

Fig. 2. SEM images of a surface texture obtained in KOH solution: (a) for Cz-Si, (b) for mc-Si

In this work as antireflection layer for solar cells the titanium dioxide layer was deposited by the chemical vapour deposition (CVD) method with tetraethylorthotitanat $(C_2H_5O)_4Ti$, using purified nitrogen as a carrier gas (Fig. 1). The liquid source $(C_2H_5O)_4Ti$ had vaporized at 200°C in a quartz bubbler and then it was transported to the Teflon nozzle (5 mm diameter) located 10 mm above the silicon wafer. The wafers were heated in the temperature range of 150°C – 400°C, at the step change of 50°C.

The Du Pont PV145 paste, for the front contact and the Ferro CN53-101 Al Conductor paste, for the back contact, were printed using 330 mesh screens. The silicon wafers, after drying at 150°C for 15 min, were co-fired in the infrared (IR) conveyor furnace, having three zones heated at temperatures 550°C, 650°C and 880°C, using the belt speed of 160 cm/min.

3. Structural and optical properties of TiO_2 and determination of a layer thickness

The crystallographic studies were performed on X'Pert MPD Phillips X-ray diffractometer in a grazing incidence configuration (GID). In this configuration the increase in the absorption path of the primary beam in a very thin layer is achieved by reducting the angle of incidence down to a few degrees. Figure 3 shows the diffraction patterns of TiO_2 films obtained at the different substrate temperature. All the layers contain anatase phase embedded in the amorphous background. As can be seen, the TiO_2 layers become more crystalline with an increase of the substrate temperature.

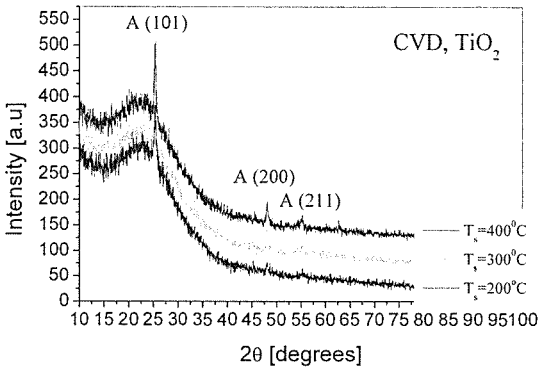

Fig. 3. The influence of substrate temperature T_s on X-ray GID patterns of TiO_2 layers. Denotation A – anatase

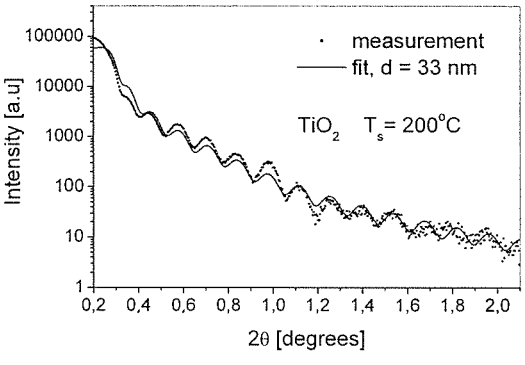

Fig. 4. Grazing incidence X-ray reflectivity (GIXR) profile for TiO_2 deposited at 200°C. The best fit to the experimental data with the fitted parameter d = 33 nm is given by solid line

The layer thicknesses were derived from grazing incidence X-ray reflectivity (GIXR) profiles for the TiO_x layers. The GIXR is a technique based on the reflection of X-ray by a flat surfaces [3]. For a thin layer on the bulk substrate (Fig. 4) the reflectivity curve exhibits periodical oscillations called Kiessig fringes. They are similar to those observed in optics, due to the interference of X-rays at each defined interface. The layer thickness is determined from the angular distance between Kiessig fringes.

Transmission T(λ) and reflection R(λ) of the TiO_x layers were measured with a Perkin Elmer U/VIS/NIR Lambda 19 spectophotometer with an integrating sphere over the wavelength range λ = 300–1300 nm (Fig. 5).

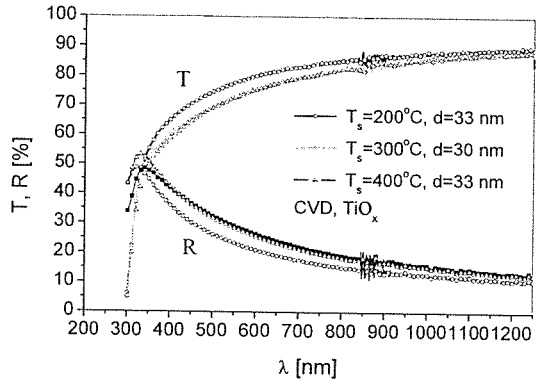

Fig. 5. The influence of the substrate temperature on the optical spectra of TiO_2 layers

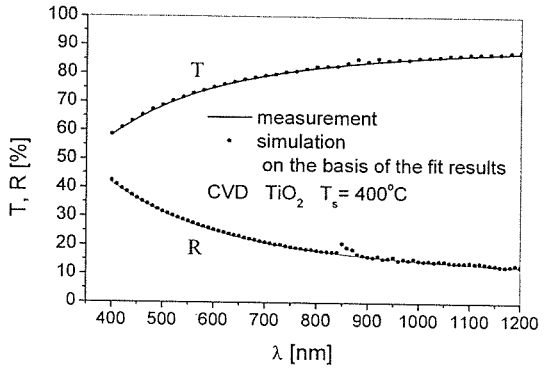

Fig. 6. Fits to experimental T(λ) and R(λ) data for the TiO_2 layer deposited at the substrate temperature T_s = 400°C

The thicknesses shown in Fig. 5 have been extracted from GIXR profiles of the TiO_x layers. The wavelength-dependent refractive index n(λ) and extinction coefficient k(λ) were determined by fitting a single layer model to the data T(λ) and R(λ). The correlation for the *n* and *k* dispersive coefficients proposed by Cauchy have been applied. The Cauchy equations are empirical formulas which are best suited to model transparent materials (e.g. TiO_2) [4]. The equations 1 and 2 define the optical constants of the Cauchy material:

$$n(\lambda) = A_n + \frac{10^6 B_n}{\lambda^2} + \frac{10^{12} C_n}{\lambda^4} \quad (1)$$

$$k(\lambda) = A_k + \frac{10^6 B_k}{\lambda^2} + \frac{10^{12} C_k}{\lambda^4} \quad (2)$$

where: λ in [nm], A_n B_n and C_n the material coefficients that define n(λ), A_k, B_k and C_k the material coefficients that define k(λ) (parameters of the fitting procedure).

The measured and fitted T(λ), R(λ) curves for one of the TiO_2 layer are shown in Fig. 6. The differences between the experimental and simulated spectra are within the measurement accuracy. The refractive index *n* and the the extinction coefficient *k* vs. *λ* show the dispersion typical for TiO_2 below the fundamental absorption edge [5]. It is particularly true for the layers obtained at the elevated substrate temperatures (T_s = 300°C, 400°C). The overall increase in *n* when the substrate temperature increases propably results from the increase in the layer density [6] (Fig. 7, 8).

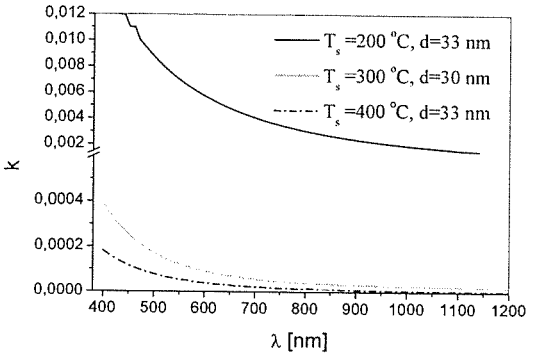

Fig. 7. Extinction coefficient *k* as a function of *λ* derived from the spectra showed in Fig. 5

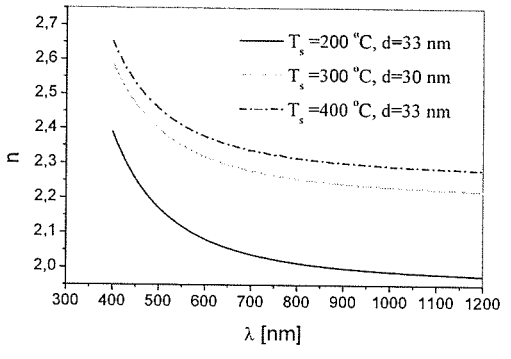

Fig. 8. Refractive index n as a function of wavelength λ

In the laboratory test for solar cell with TiO_2 ARC the best value of refractive index *n* has the layer deposit-

ed at 400°C but for solar cells laminated in PV module, where there are capped with glass, the n closed to 2 for the wavelengths longer than 450 nm is more optimal.

4. Measurements of solar cells electrical parameters

The I-V characteristics of solar cells were measured under standard test condition i.e. light spectrum AM1.5G, normalized to 1000 W/m^2 and 25°C cell temperature and the final data are collected in Tab. 1. A reference cell was calibrated at Wrocław University of Technology in Photovoltaic Laboratory Solar Lab using B-class Sun simulator.

TABLE 1

The I-V parameters of the solar cells in dependence on TiO_2 deposition temperature and surface texture

Cell No.	Deposition temperature [°C]	I_{sc} [mA]	V_{oc} [mV]	R_{sh} [Ω]	R_s [mΩ]	P_m [W]	FF	E_{ff} [%]
Cz-Si (100) – regular piramidal texture								
1	150	869	599	10.25	16.4	374	0.719	14.92
2	200	870	600	18.36	15.1	384	0.736	15.32
3	250	873	601	36.68	17.4	393	0.749	15.68
4	300	872	601	32.26	18.1	391	0.746	15.60
5	350	846	599	48.60	19.8	389	0.767	15.50
6	400	837	597	55.04	21.6	382	0.765	15.25
mc-Si – random geometrical figures texture								
7	150	528	580	2.33	79.0	124	0.410	5.01
8	200	757	582	12.61	10.1	293	0.665	11.67
9	250	752	580	16.67	18.2	295	0.676	11.76
10	300	765	590	19.35	21.6	289	0.641	11.53
11	350	745	578	18.51	18.2	292	0.678	11.63
12	400	729	578	33.43	39.4	297	0.704	11.65

where: I_{sc} – short circuit current, V_{oc} – open circuit voltage,
R_{sh} – shunt resistance, R_s – series resistance,
P_m – power in optimum point, FF – fill factor,
E_{ff} – conversion efficiency.

The cells numbered from 1 to 6 have homogenous surface texture presented in Fig. 2a. For the cells numbered from 7 to 12 only one example of the surface texture is presented in Fig. 2b due to random crystallographic orientation of the particular grains.

The present results indicate that the electrical parameters of the silicon solar cell depend on the temperature of the TiO_2 deposition. The CVD process performed at 250°C leads to the best photoconversion efficiency. For the lower deposition temperature of TiO_2, the obtained V_{oc} and R_{sh} values suggest, that the TiO_2 layer does not protect effectively p-n junction from penetration of silver atoms. However, above 250°C, the presence of the crystalline phase of anatase (as shown in Fig. 3) makes the metallization process more difficult which results in the lowering I_{sc} and increasing R_s values and consequently leads to the photoconversion efficiency decrease.

5. Conclusions

The evolution of the crystallographic structure with the substrate temperature for the TiO_2 layers containing anatase phase embedded in the amorphous background has been shown. A progress of the crystallization process with the increasing temperature of the substrate during the TiO_2 deposition by CVD method has been observed. The process performed at 250°C leads to the best photoconversion efficiency. This is a compromise between protection and antireflection role of TiO_2 layer in silicon solar cell structure. The effect is the same for the monocrystalline silicon solar cells with regular piramidal texture of the surface and for the multicrystalline silicon solar cells with random geometrical figures texture. From an optical point of view the best antireflection properties has the TiO_2 layer deposited at 400°C, with k coefficient near to zero.

Acknowledgements

This work was supported by the POLISH ECO-ENERGY NETWORK 2007 program.

REFERENCES

[1] P. Maycock, T. Bradford, PV Market Update: Demand Grows Quickly and Supply Races to Catch Up, www. Renewable-energy-world.com, **10**, 2007.

[2] P. Panek, M. Lipiński, E. Bełtowska-Lehman, K. Drabczyk, R. Ciach, Industrial Technology of Multicrystalline Silicon Solar Cells, Opto-Electr. Rev. **11**, 4, 269-275, 2003.

[3] P. F. Fewster, X-ray Analysis of Thin Films and Multilayers, Rep. Prog. Phys., **59**, 1339-1407, 1996.

[4] J. H. Simmons, K. S. Potter, Optical Materials, Academic Press, 2000.

[5] N. Ozer, H. Demiryoatt, J. H. Simmons, Appl. Opt. **30**, 3661, 1991.

[6] K. Okima, Low Temperature Growth of Rutile TiO_2 Films in Modified rf magnetron sputtering, Surf. Coat. Technol. **135**, 286, 2001.

Received: 3 December 2007.